



HAL
open science

Discovery of Mega-Sheath Folds Flooring the Liwan Subbasin (South China Sea): Implications for the Rheology of Hyperextended Crust

C. Zhang, G. Manatschal, X. Pang, Z. Sun, J. Zheng, H. Li, L. Sun, J. Zhang,
Y. Zhao

► To cite this version:

C. Zhang, G. Manatschal, X. Pang, Z. Sun, J. Zheng, et al.. Discovery of Mega-Sheath Folds Flooring the Liwan Subbasin (South China Sea): Implications for the Rheology of Hyperextended Crust. *Geochemistry, Geophysics, Geosystems*, 2020, 21 (7), 10.1029/2020GC009023 . hal-03102387

HAL Id: hal-03102387

<https://hal.science/hal-03102387>

Submitted on 7 Jan 2022

HAL is a multi-disciplinary open access archive for the deposit and dissemination of scientific research documents, whether they are published or not. The documents may come from teaching and research institutions in France or abroad, or from public or private research centers.

L'archive ouverte pluridisciplinaire **HAL**, est destinée au dépôt et à la diffusion de documents scientifiques de niveau recherche, publiés ou non, émanant des établissements d'enseignement et de recherche français ou étrangers, des laboratoires publics ou privés.

Copyright

Geochemistry, Geophysics, Geosystems

RESEARCH ARTICLE

10.1029/2020GC009023

Key Points:

- Sheath folds in seismic basement flooring the Liwan subbasin developed weak, forearc inherited anisotropic metasediments
- Metasediments derived from midcrust levels were unroofed in the footwall of an extensional detachment fault during hyperextension
- Combination of a pure shear and a simple shear regime accounts for the extreme thinning of the crust underneath the Liwan subbasin

Correspondence to:

C. Zhang,
cmzhang@scsio.ac.cn

Citation:





Zhang, C., Manatschal, G., Pang, X., Sun, Z., Zheng, J., Li, H., et al. (2020). Discovery of mega-sheath folds flooring the Liwan subbasin (South China Sea): Implications for the rheology of hyperextended crust. *Geochemistry, Geophysics, Geosystems*, 21, e2020GC009023. <https://doi.org/10.1029/2020GC009023>

Received 6 MAR 2020

Accepted 5 MAY 2020

Accepted article online 8 MAY 2020

Discovery of Mega-Sheath Folds Flooring the Liwan Subbasin (South China Sea): Implications for the Rheology of Hyperextended Crust

C. Zhang^{1,2} , G. Manatschal³ , X. Pang^{4,5}, Z. Sun^{1,2} , J. Zheng^{4,5}, H. Li^{4,5}, L. Sun^{1,2}, J. Zhang⁶ , and Y. Zhao^{7,8}

¹CAS Key Laboratory of Ocean and Marginal Sea Geology, South China Sea Institute of Oceanology, Guangzhou, China,

²Innovation Academy of South China Sea Ecology and Environmental Engineering, Chinese Academy of Sciences,

Guangzhou, China, ³IPGS/CNRS, Université de Strasbourg, Strasbourg Cedex, France, ⁴CNOOC Ltd.-Shenzhen,

Shenzhen, China, ⁵CNOOC Ltd.-Deepwater, Shenzhen, China, ⁶The Chinese University of Hong Kong, Shenzhen, China,

⁷Key Laboratory of Submarine Geosciences, State Oceanic Administration, Hangzhou, China, ⁸Second Institute of

Oceanography, Ministry of Natural Resources, Hangzhou, China

Abstract Sheath folds recognized on kilometer scale are rare and only described in salt tectonics in seismic data. Here, we present mega-sheath folds spectacularly imaged in a 3-D seismic survey in the seismic basement flooring the hyperextended Liwan subbasin in the northern margin of the South China Sea. The sheath folds show eye structures delimited by anastomosing discontinuities. The axial planes of the sheath folds are subparallel to a rift-related, extensional detachment surface separating hyperextended seismic basement from the syn-rift sedimentary sequence. The sheath folds as well as the anastomosing discontinuities formed during hyperextension by ductile shearing of the forearc inherited and prestructured metasediments. The ductile shearing eventually resulted in the metasediments derived from midcrust unroofed at the footwall of an extension detachment fault. The discovery of mega-sheath folds and ductile deformation within the basement conflicts with the general assumption that hyperextended domains are in the brittle field. The new seismic observations show the importance of forearc inherited, prestructured anisotropic basement controlling the crustal rheology during hyperextension.

Plain Language Summary A wealth of research has established the classic crustal model with a strong brittle upper crust and a weak ductile lower crust. The styles of deformation depend on rheological and mechanical properties of the materials and generally exhibit brittle faulting in the upper crust and ductile flow in the lower crust, respectively. However, remarkable changes in the crustal rheology and mechanics can occur in strongly inherited, complex geological settings, which up to date have not been well established. In this study, we present and discuss the occurrence of mappable sheath folds generated under high ductile shear strain in metasediments in the basement, and we decipher the questions of when, how, and in what conditions these structures formed. Our results demonstrate that these mega-sheath folds formed within a forearc inherited anisotropic basement, and the rocks are derived from midcrustal levels. During hyperextension, they were unroofed in the footwall of a major extensional detachment. Ductile deformation and shearing became responsible for the extreme thinning of the crust.

1. Introduction

Sheath folds are characterized by highly curvilinear hinges that progressively rotate from high angles into parallelism with the transport direction (Carreras et al., 1977). Most sheath folds are recognized on the centimeter to meter scale, while examples on the kilometer, seismic scale are rare (Fiduk & Rowan, 2012; Lacassin & Mattauer, 1985). Kinematics and mechanisms of sheath fold formation are well documented (e.g., Alsop & Holdsworth, 2006). The supposed deformation regimes in which sheath folds form are shearing and/or constriction and flattening related to the flow of weak/ductile materials (Ez, 2000; Searle & Alsop, 2007). Sheath folds can, however, also result from poly-phase deformation in which case they overprint inherited structures.

Here, we discuss the implications of megascopic folds observed in high-resolution, 3-D seismic sections in metasediments belonging to the seismic basement that floors the hyperextended Liwan subbasin (i.e.,

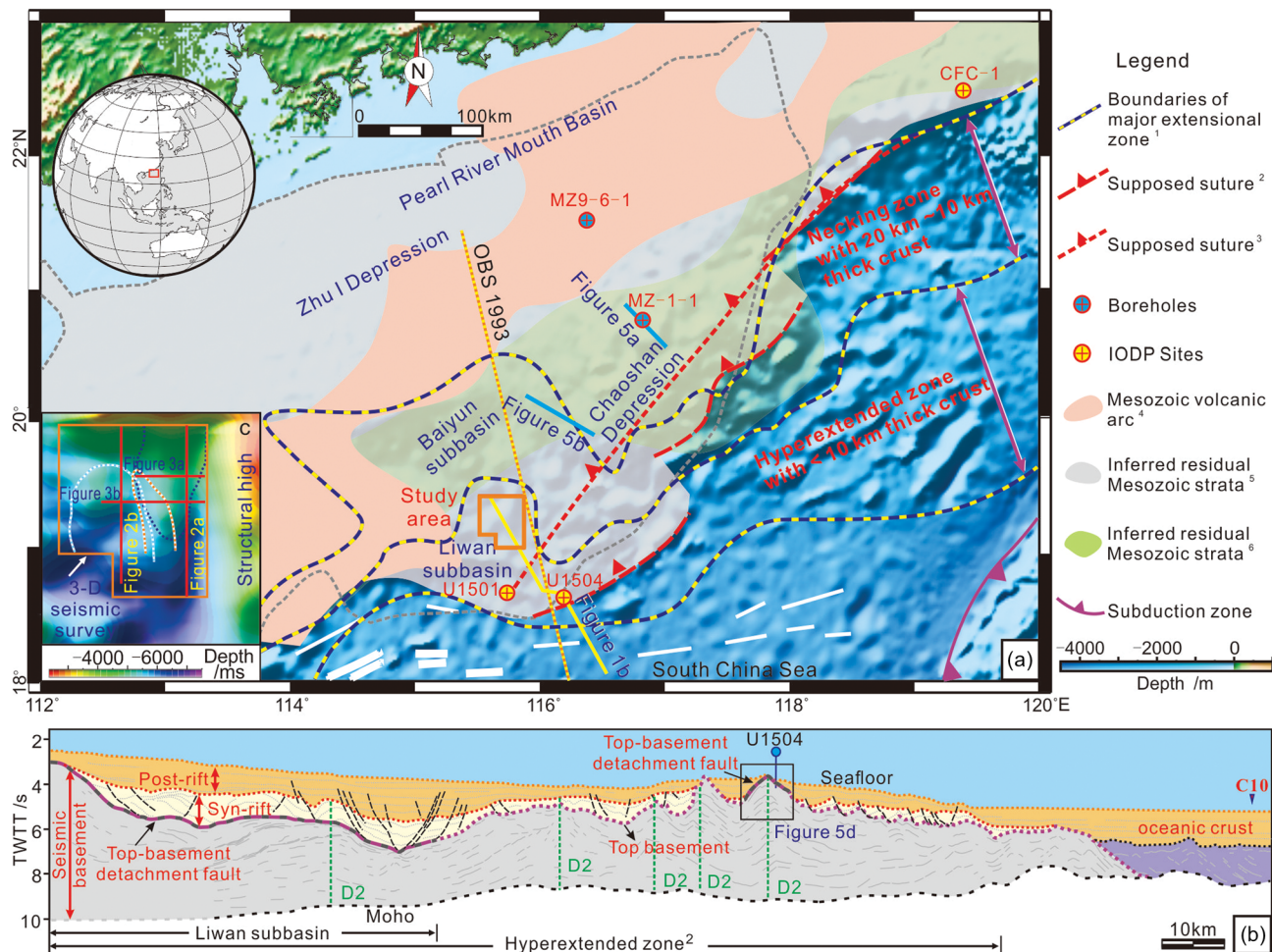


Figure 1. Regional setting and projection of sheath folds in the study area. (a) Bathymetric map showing the location of the study area and forearc inherited setting on a regional scale. (b) Interpreted seismic reflection profile showing the top of the basement flooring the syn-rift faults in the Liwan subbasin (Zhang et al., 2019), as well as the large-scale structural configuration of the distal margin. IODP site U1504 in the distal margin cored the basement and recovered the mylonites (Larsen et al., 2018b). Note the segments of the top basement in the Liwan subbasin and in the drilling area of site U1504 were interpreted as detachment faults (Sun, Sun, et al., 2019; Zhang et al., 2019). The green dashed lines mark the axial planes of D2 folds, which are related to magmatic additions (Sun, Lin, et al., 2019). (c) Inset map showing the different vergence by projecting the enveloping lines of axial hinge zones of D1 folds in the 3-D seismic survey. The base map shows the depth of the top of seismic basement. Bathymetry reproduced from the GEBCO world map, <http://www.gebco.net> data. Data sources: 1—Yang et al. (2018); 2—Zhou et al. (2006); 3—Holloway (1982); 4—Li et al. (2018); 5—Sun et al. (2014); 6—Hu et al. (2015).

thinned to less than 10 km by definition of Peron-Pinvidic et al., 2013), which is located in the distal Pearl River Mouth basin in the northern South China Sea (SCS). The discovery of mega-sheath folds in a distal margin is important since it allows us to reexamine the crustal rheology and mechanisms of crustal thinning in hyperextended domains commonly assumed to be brittle and controlled by detachment faults as demonstrated from the archetype, hyperextended Iberia rifted margin (e.g., Nirrengarten et al., 2016).

Regional studies (e.g., Yao et al., 1994; Zhou et al., 1995, 2006) indicated that the northern SCS developed over a fossil subduction setting associated with the Mesozoic paleo-Pacific active margin (Li et al., 2014; Zahirovic et al., 2014). Extension caused by slab rollback (Schlüter et al., 1996; Zhou et al., 1995) and slab pull (Hall, 1996; Sun et al., 2006) is believed to have started during the Late Cretaceous, before the multiple episodes of rifting resulted in lithospheric breakup and the onset of seafloor spreading in early Oligocene (Ru & Pigott, 1986). The preexisting Mesozoic granitoids, metasediments, and compressional structures have been interpreted to develop in a suprasubduction setting bearing a strong subduction inheritance, well documented throughout the Pearl River Mouth basin in industry wells and seismic data (Shao et al., 2007; Shi & Li, 2012; Wu et al., 2007; Yan et al., 2014; Ye et al., 2018). According to paleogeographic reconstructions (e.g., Holloway, 1982; Shao et al., 2017; Zhou et al., 2006; Figure 1a), the Liwan subbasin developed above the

Mesozoic paleo-Pacific suture zone including Mesozoic forearc material, corresponding to a mechanically weak basement (Li et al., 2014; Prucha, 1992). Extension resulted in hyperextended crust flooring the Liwan subbasin (Zhang et al., 2019; Yang et al., 2018; Figures 1a and 1b); however, the mechanism of crustal thinning is still controversial. Previous studies interpreted low-angle detachment faults offsetting the basement to accommodate the extreme crustal thinning below the Liwan subbasin (Larsen et al., 2018c; Lei et al., 2019). Based on the new data set, this study shows evidences about the detachment fault and the architecture of the basement, which enable to address that the crustal hyperextension was probably achieved by the combination of simple shear along this top-basement detachment and pure shear of weak, prestructured metasedimentary layers inherited from a forearc setting. The most prominent level, well imaged in seismic sections, resulted from the detachment between syn-rift sediments and seismic basement (Figure 1c; Zhang et al., 2019).

This study aims to describe the occurrence of exceptionally well preserved and seismically imaged mega-sheath folds in the seismic basement flooring the Liwan subbasin, to decipher the heterogeneity of forearc-inherited seismic basement in which these folds developed, to explore the nature and rheology of the basement, and to discuss the mechanism of mega-sheath fold formation and mechanical implications for the evolution of hyperextended rifted margins.

2. Data and Methods

This study is based on a high-resolution depth-migrated 3-D seismic data set (BLK4311), which is released for the first time, making the Liwan subbasin an ideal place to correlate structures and interfaces on a basin scale. The seismic data set was acquired by the China National Offshore Oil Corporation (CNOOC) from 2002 to 2012. The 3-D seismic data covers the major Liwan subbasin, with a total surface area of 1,600 km² (Figure 1c). The volume was processed to a main frequency bandwidth of 30–45 Hz. The record to 10 km depth provides high-quality imaging of the structures in the basement, which cannot be observed in the time-migrated 2-D seismic data. The trace interval is 12.5 m. The high-density time-migrated 2-D seismic profile crosses the Liwan subbasin and extends onto the first oceanic crust, which is used to constrain the interpretation of the Moho (Figure 1b). The seismic basement is referred to herein as the seismic package flooring the syn-rift sequence.

Industrial wells and International Ocean Discovery Program (IODP) Sites, which penetrated seismic basement, are presented in this study, together with the seismic sections passing through these wells. Site U1501 from IODP Expedition 368 is located over the Outer Marginal High (OMH) (Figure 1a), which forms the seaward boundary of the Liwan subbasin. The top of the basement corresponds to the most prominent unconformity in the Pearl River Mouth basin, which is due to the juxtaposition of lithologies with contrasting physical properties (Larsen et al., 2018a), also referred to as “top of seismic basement.” IODP Site U1504 cored the basement of another OMH in the more distal margin and recovered greenschist mylonites overlain by the late Eocene syn-rift sediments (Larsen et al., 2018b). Macrostructure and mineral analysis suggest that the mylonites experienced mainly normal ductile shearing and is supposed to be exhumed from midcrust during Cenozoic extension (Sun, Lin, et al., 2019). Thus, the top of seismic basement corresponds to a stratigraphic unconformity and/or a detachment surface.

Based on the description and interpretation of new high quality, depth-migrated seismic data, we identify and describe fabrics and structures in the seismic basement that floors the Liwan subbasin. We have correlated them in the 3-D seismic survey in order to explore their geometrical variation. A comparison in terms of reflectivity, velocity and structures between the basement flooring the hyperextended Liwan subbasin and the adjacent drilled areas aims to constrain the nature of the basement in the study area. The syn-rift sequence boundaries used in this study have been described in previous studies (Zhang et al., 2019).

3. Results

In dip lines of the 3-D seismic survey (Figure 2), high-amplitude, continuous reflectors are observed in the hyperextended basement. Only few faults observed in the syn-rift sequence penetrate into the seismic basement, which is capped by high-amplitude reflectors interpreted to represent an extensional detachment fault (Zhang et al., 2019). In the footwall of this fault, two sets of folds are recognized in the seismic data referred

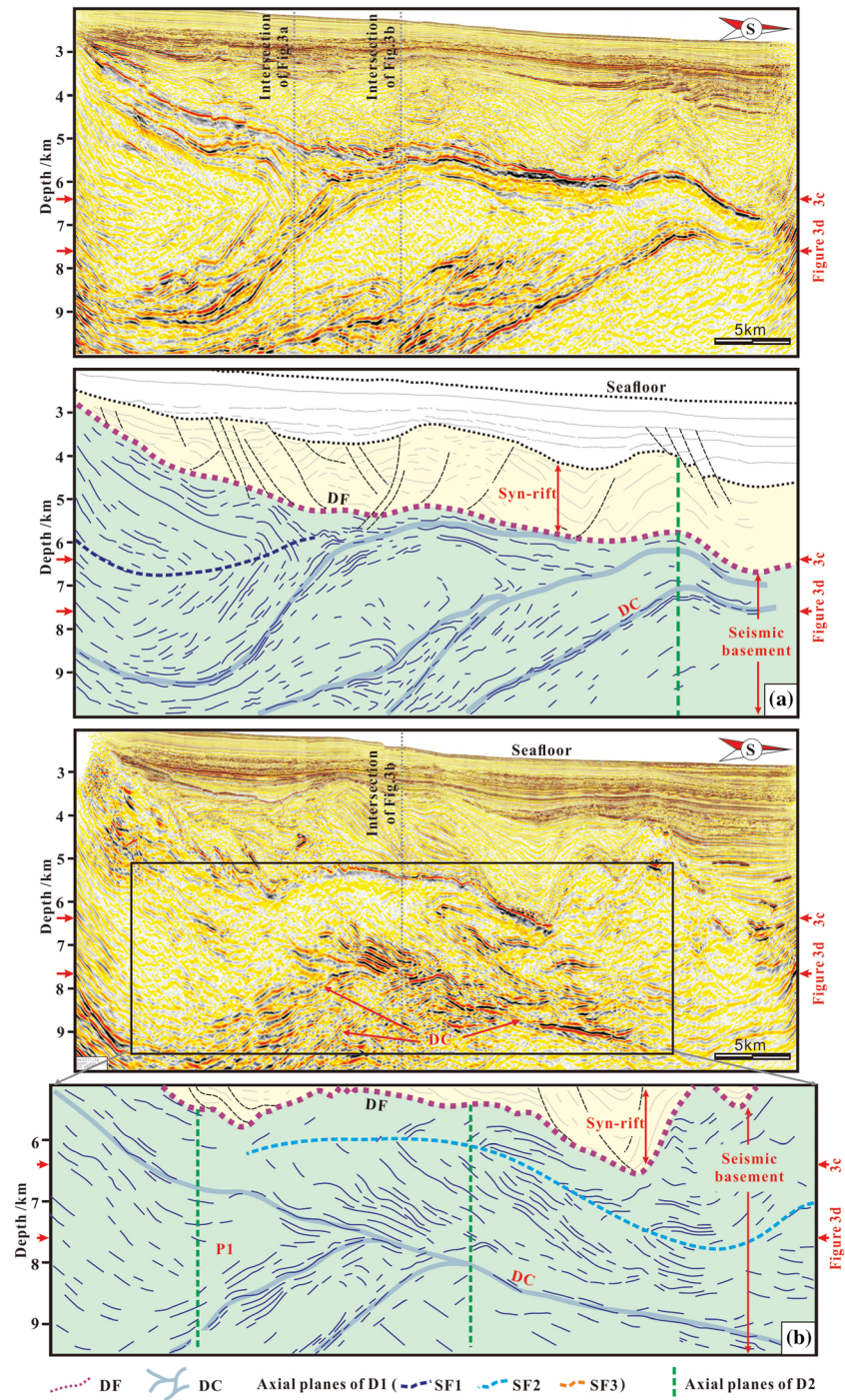


Figure 2. Depth-migrated seismic reflection images and related interpretation showing folds and discontinuities in the seismic basement that is separated from the overlying syn-rift sequence by a major, rift-related detachment fault. (a) SF1 (D1 fold) showing seaward vergence and axial planes merging with the top-basement detachment fault. (b) SF2 with continentward vergence superimposed by D2 and discontinuities showing anastomosing in the seismic basement. DF—detachment fault; DC—discontinuities; SF—sheath fold; P1—Package 1. See Figure 1c for locations.

to as D1 and D2, respectively. D1 consists of three, kilometer-scale mappable sheath folds, referred to as SF1, SF2, and SF3. The axial planes of D1 folds are overprinted by a second fold generation referred to as D2 folds. SF1 and SF2 show ocean- and continent-ward vergence, respectively (Figure 2). SF1, up to 6 km thick, occurs in the northernmost section, while SF2 can be observed over 25 km in the dip section with thickness of about

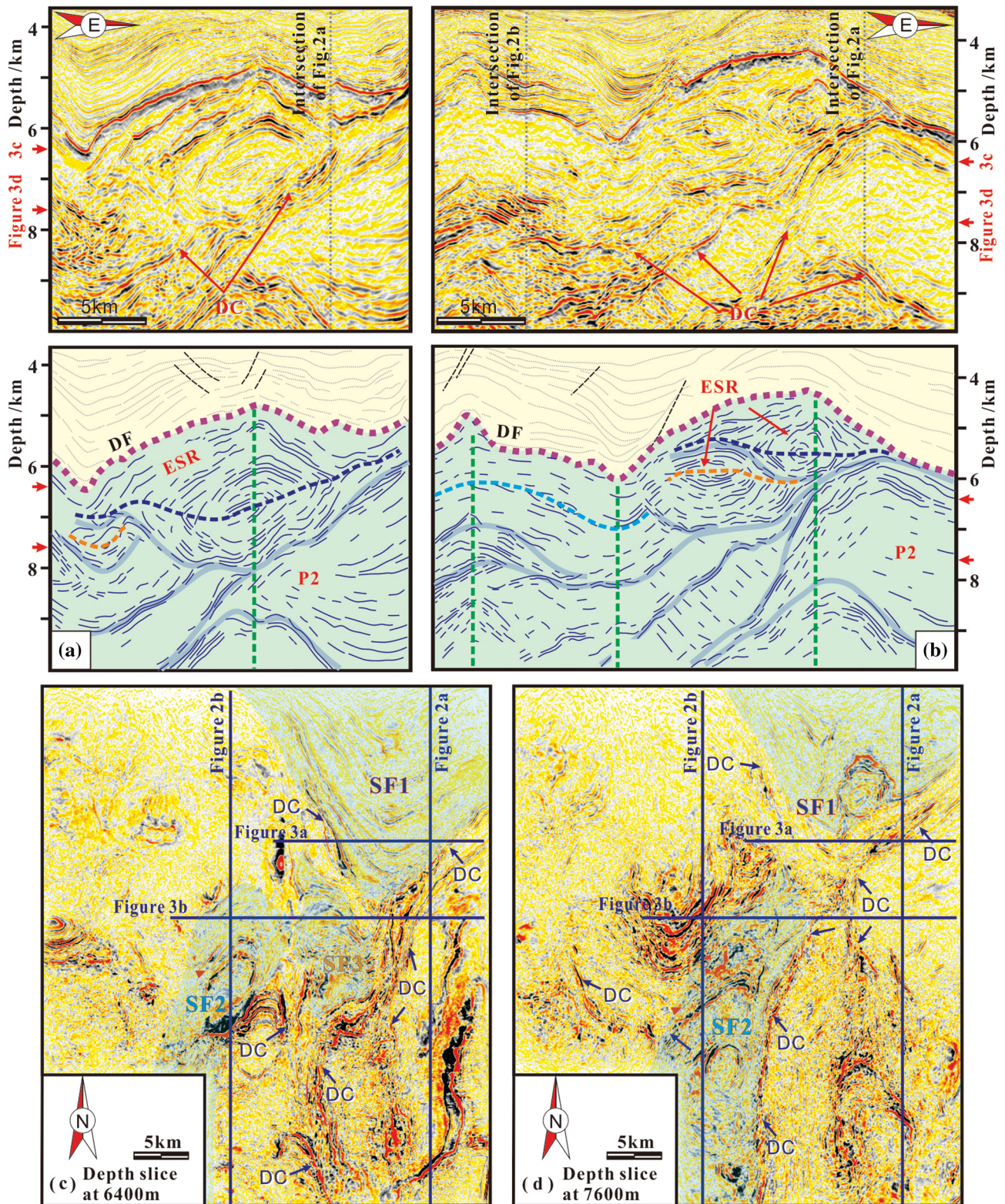


Figure 3. Depth-migrated strike lines and depth slices extracted from the 3-D seismic data showing the interpretation of folds and discontinuities. (a) D1 folds with axial planes subparallel to the detachment fault superimposed by D2. (b) Eye-shape rings of D1 and anastomosing discontinuities in the seismic basement. Depth slices at 6,400 m (c) and at 7,600 m (d) showing the view of the anticlines, different packages and anastomosing discontinuities. D1 folds are highlighted in light green. ESR—eye-shape ring; P2—Package 2. More abbreviations follow those given in Figure 2.

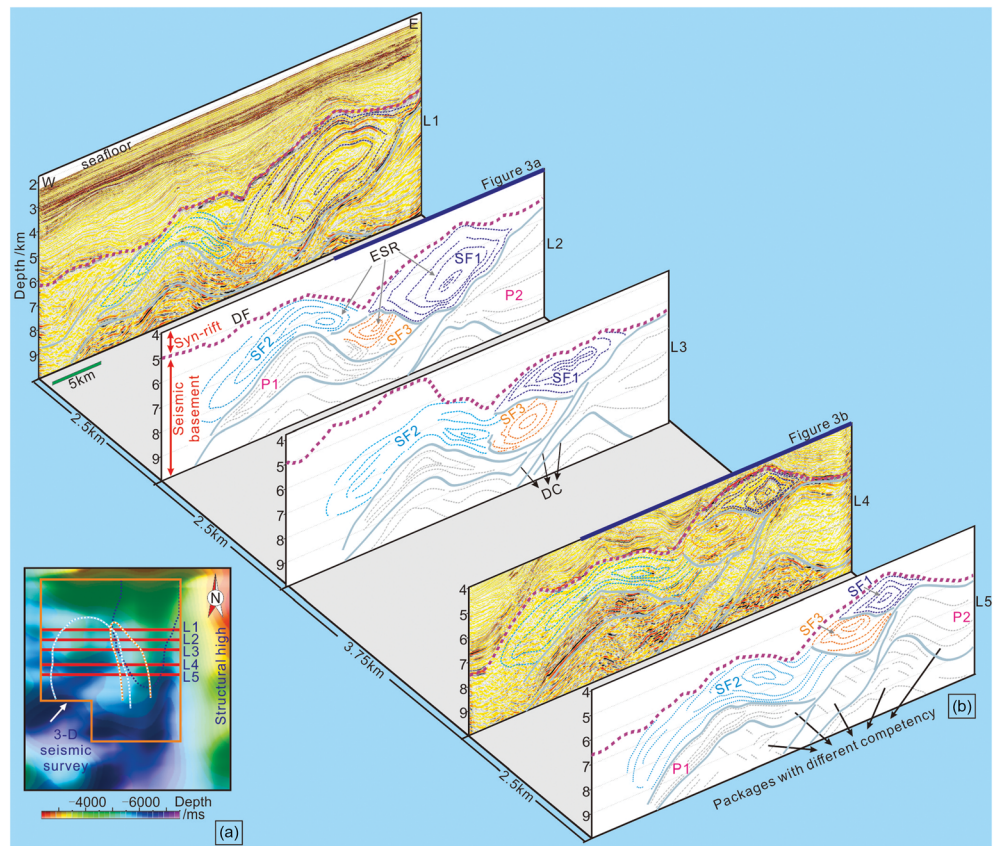


Figure 4. View of five W–E directed strike lines showing the 3-D geometry of the sheath folds (SF1, SF2, and SF3) and the top-basement detachment faults. (a) The locations of the seismic lines extracted from a 3-D seismic survey. (b) Three-dimensional geometries of the three sheath folds and the anastomosing discontinuities delimiting the packages in the seismic basement. The dashed purple lines mark the detachment faults separating the upper syn-rift sequence from the lower seismic basement. The dashed gray lines show the layering in each package, either perpendicular or parallel or oblique to or converging toward the associated discontinuities.

2.5 km. The axial plane of SF1 merges into the top-basement, syn-extensional detachment fault (Figure 2a), while the axial plane of SF2 is subparallel to slightly oblique to the detachment fault (Figure 2b). The outer layers enveloping D1 folds are characterized by high-amplitude reflections, which are geometrically concordant with the layers with low-amplitude reflection below SF1, or oblique to the layers below SF2. Such high-amplitude reflectors wrapping packages with characteristic geometry and reflectivity are defined as discontinuities. In E–W strike lines, well imaged eye-shaped rings define the noses or caps of large D1 sheath folds (Figures 3 and 4). The axial planes of the sheath folds are subparallel to the extensional detachment fault. The eye-shaped rings of SF1, however, are contorted and progressively thin toward the east and west. The hint of SF3 is visible in Figures 3b and 4 as ring structures.

It is notable that in the whole seismic basement, the discontinuities are ubiquitous, not only delimiting the folds from the surrounding layers, but divide the basement into different packages showing a variety of amplitude and continuity of reflections. Each package presents diagnostic fabrics, in which the layers are either parallel or perpendicular or oblique to the associated discontinuities (Figures 2 and 3a and 3b). Packages (e.g., P1 and P2) strikingly thinning toward the converging discontinuities present shapes similar to sheath folds, but no eye-shaped rings can be observed (Figure 4). There is no evidence for truncations between intrabasement anastomosing discontinuities separating sheath folds and the major extensional detachment capping the seismic basement.

Depth slices at 6,400 m and 7,600 m illustrate the relationship of sheath fold and discontinuities (Figures 3c and 3d). The shallower depth slices cut through the main body of the three sheath folds. The patterns of three

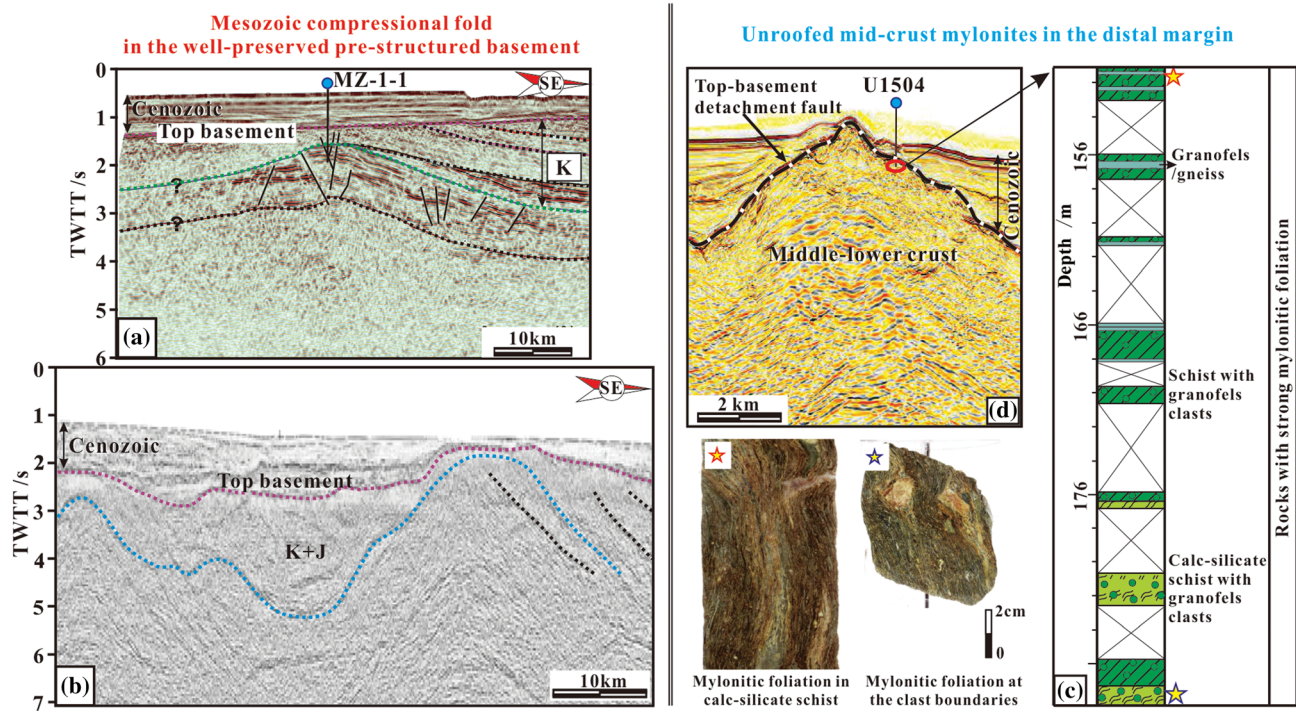


Figure 5. Well-preserved prestructured anisotropic basement and drill hole evidence for the occurrence of ductile deformation in the seismic basement outside the Liwan subbasin. (a) Well MZ-1-1 and wide open anticline in the proximal margin (Li et al., 2008); (b) well-preserved compressional folds in the seismic basement of the Chaoshan Depression (Yan et al., 2014), together with a, showing the prestructured forearc-inherited anisotropic basement. (c) Mylonites comprising the seismic basement from IODP site U1504 drilled south to the Liwan subbasin in the distal margin and strong mylonitic foliation observed in the calc-silicate schist and around the granofels clasts (Larsen et al., 2018b); (d) the mylonites deriving from middle-lower crust were exhumed at the footwall of the top-basement detachment fault (Sun, Lin, et al., 2019); however, the extent and geometry of the detachment fault is still unclear. TWTT—two-way travel time. K—Cretaceous; J—Jurassic; please see Figures 1a and 1b for the locations of wells and seismic sections.

anticlines can be observed bordered by discontinuities. Hints for other anticlines can be seen in the slices; however, they are not really traceable in the seismic profiles. This is either due to poor-continuity, to low-amplitude reflection or limited scale of the structures. In the deeper slice, only the anticlines of SF1 and SF2 are present. All fabrics together with related discontinuities are highly contorted and display the strong heterogeneity of the seismic basement. A 3-D view shows the lateral changes in geometries of the sheath folds and discontinuities (Figure 4), SF1 closes oceanwards, becoming smaller from section L1 toward L5. SF2 and SF3 close in the opposite direction.

These D2 folds represent coaxial upright folds (Figures 1b and 2). In the section, the axial planes of D1 and D2 folds are subperpendicular, which also explain the classical dome and basin type interference pattern seen in Figures 3c and 3d (Ramsay & Huber, 1987). The antiforms of D2 folds present limited and isolated distribution. In addition, D2 folds are cored by symmetric pull-up geometries rooting at depth. The deformed extensional detachment caps the seismic basement as well as the overlying syn-rift sediments (Figures 1b and 2a). D2 folds have been interpreted to be related to the emplacement of laccolith intrusions during hyperextension (Zhang et al., 2019).

4. Discussion

4.1. Nature of Mega-Sheath Folds and Role of Inherited Weak Metasediments

The reflectors comprising these sheath folds and underlying packages appear as well-layered and continuous reflections in the seismic basement and correspond to velocities of 5.0–5.5 km/s according to correlations with the OBS data reported by Yan et al. (2001). This indicates that they do not likely represent crystalline quartzo-feldspatic crust, which rarely show layered and continuous reflectivity and velocities <6.0 km/s.

Previous studies of seismic data and numerous wells suggest that Mesozoic strata are widely distributed in the northern SCS (e.g., Li et al., 2008; Figure 1a). Outside the Liwan subbasin, well MZ-1-1 in the Chaoshan Depression penetrated into seismic basement and recovered Early Cretaceous terrestrial and Jurassic marine clastic sequences (Shao et al., 2007; Wu et al., 2007; Li et al., 2008; Figure 5a; for location, see Figure 1a). The velocities of Mesozoic strata calculated from multichannel seismic and determined from well MZ-1-1 in the neighboring Chaoshan Depression are in the range of 3.5–5.5 (Fan et al., 2019), or 4.4–5.4 km/s (Ruan et al., 2009), that is, slightly lower than those found in the seismic basement flooring the Liwan subbasin. At IODP Site U1504, greenschist mylonites interlayered with granofels recovered in the seismic basement has a velocity of 5.0–6.1 km/s (Larsen et al., 2018b) and its highly oriented gneiss-like lineation observed in the samples is consistent with the weak to intermediate continuous intrabasement lineation reflection in the profiles (Figures 2 and 3). These rocks may be analogs to the rocks forming the folded basement that floors the Liwan subbasin. We therefore conjecture that the sheath folds might be developed in metasediments.

In the section across well MZ-1-1, wide and open anticlines were observed (Li et al., 2008; Figure 5a), which were inferred to develop in the hanging wall of the NW-verging subduction of the Late Mesozoic Pacific Plate by Yan et al. (2014) during latest Jurassic to Early Cretaceous. Subduction-related compressional folds with wavelength of up to 20 km are also observed in metasediments in the seismic basement overlying a more than 15-km-thick crystalline crust (Yan et al., 2014; Figure 5b). In the Zhu I Depression, thrust faults are preserved in the seismic basement unconformably covered by syn-rift sediments (Ye et al., 2018). These observations suggest that the seismic basement was already deformed prior to extension. The preextensional structures in the metasediments may have resulted in strongly anisotropic, weak layers within the basement. The presence of anastomosing discontinuities in this study, reminiscent of shear zones, provides evidence for strong rheological contrasts within the heterogeneous seismic basement, which suggest that sheath fold formation may occur simultaneously with shearing and extension. The discontinuities may correspond to compositional variations and/or preexisting weak zones and/or shear zone in connection with the extension. However, the ductile deformation is unlikely to occur at the seafloor or just below the syn-rift sediments as we observed now. Thus, the ductile deformation within the hyperextended basement suggests a different mechanism from the well-preserved compressional folds related to the subduction. The most likely interpretation of the sheath folds is that they may have formed at midcrustal level as well, similar to the mylonites under greenschist facies conditions at Site U1504 (Figures 5c and 5d; Larsen et al., 2018b). The mylonitic foliation in the schist or around the granofel clasts indicates the occurrence of ductile deformation before being exhumed (Figure 5c).

A thermal overprint during hyperextension could not only explain the ductile deformation, but also the higher velocities, which is the reason why these metasediments are interpreted as part of the seismic basement. The relation between the thermal conditions and the creation of such ductile structures has been proposed based on the mylonite samples recovered at IODP Site U1504 by Sun, Lin, et al. (2019). The temperature of ductile deformation determined for these mylonites is in the range between 300°C and 400°C, evidenced from the extensive development of bulging recrystallization of quartz, microscopic fractures, and fine granulation of albite. This result can be comparable to the thermal evolution of other hyperextended systems. Direct access to pre-rift sediments from the Mesozoic Pyrenean hyperextended basins show evidence for high temperatures in excess of 400°C (T_{max}) reached during hyperextension based on Raman Spectroscopy on carbonaceous material (Clerc et al., 2015). Vacherat et al. (2014) and Hart et al. (2017) proposed paleothermal gradients for these basins ranging between 80°C/km and 100°C/km during hyperextension, based on detrital zircon fission track and (U–Th–Sm)/He, and detrital zircon (U–Th)/He thermochronology. Modeling of the thermal evolution established by Lescoutre et al. (2019) supported such high heat flow values during hyperextension. Like the Liwan subbasin, the Pyrenean hyperextended basins showed high sedimentation rates during hyperextension. These studies suggest that the thermal conditions related to hyperextension can explain ductile deformation, which is compatible with the discovery of the sheath folds in the seismic basement flooring the Liwan subbasin.

4.2. Origin and Mechanism of Sheath Fold Formation

Sheath folds can result either from monophasic or polyphasic shearing (Alsop et al., 2007; Rosas et al., 2002) and can occur either in subduction (Searle & Alsop, 2007) or extensional settings (Zuber et al., 1986). Timing and setting of sheath fold formation can therefore be related to three potential scenarios:

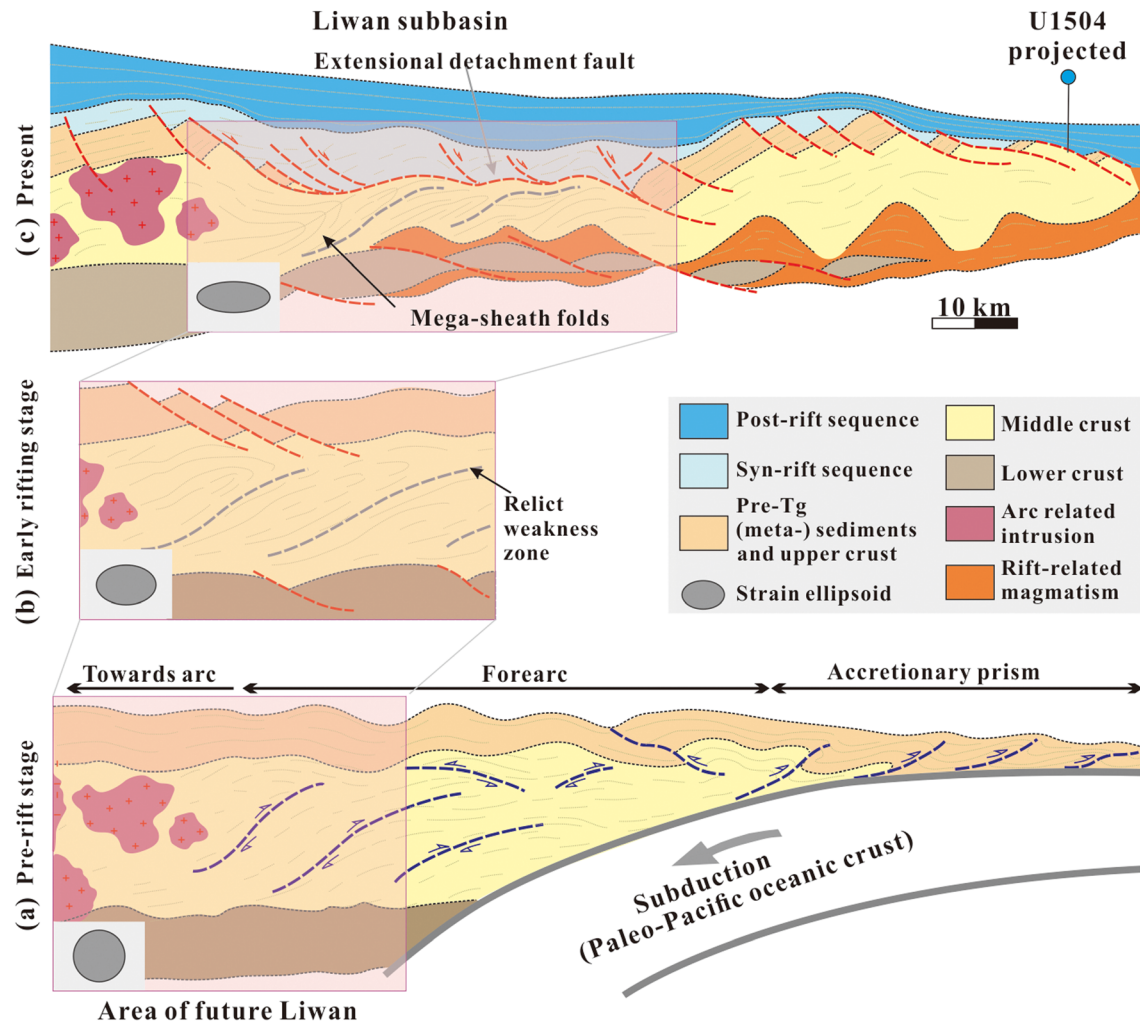


Figure 6. Conceptual model showing the origin of sheath folds and the role of inheritance on the midcrustal exhumation underneath the Liwan subbasin. (a) A conceptual section during the pre-rift stage through the paleo-Pacific active margin and location of the future Liwan subbasin. A weak, prestructured anisotropic basement was formed during the subduction. (b) A section showing the extensional deformation as well as the ductility of the prestructured basement during the early rifting stage. (c) Schematic section across the present Liwan subbasin showing the metasediments and ductile deformation deriving from the midcrust levels were exhumed along the top-basement simple shear detachment fault, as the stronger and more brittle portions of the shallow crust were offset and removed. Combination of a pure shear and simple shear regime may account for the extreme thinning of the crust. Such exhumation of the midcrust has been attested by the drilling result of IODP site U1504 in the more distal margin. The purple squares of Liwan area have the same surface and the ellipsoids are in the same relation.

(i) monophasic during subduction, (ii) monophasic during hyperextension, or (iii) polyphasic refolding preexisting, inherited folds.

In Scenario (i), the sheath folds are pre-dating hyperextension and are therefore not expected, as observed, to be synchronous and kinematically linked to the fault contact, which separates the folded seismic basement from the overlying syn-rift sediments. A subduction-related origin is also unlikely because all observed contractional deformation structures observed in the surroundings of the Liwan subbasin do not show evidence for sheath folds, as expected for forearc settings (see Figure 5a). In Scenario (ii), the geometry of sheath folds depends on the relative orientation of preexisting anisotropies with regard to the flow eigenvectors, strain magnitude, and the vorticity of the flow (Reber et al., 2012). Folds can only form if anisotropic layers (reflections) that were before folding within the shortening field of the strain ellipsoid; that is, they could not be sub-horizontal. That is to say, the occurrence of a pre-extensional, anisotropic basement is required. Thus, the most plausible scenario is that sheath fold formation is controlled by inherited structures in a weak and strongly anisotropic basement favoring Scenario (iii).

Furthermore, the anastomosing discontinuities separating the strongly anisotropic packages may represent inherited structures within the weak metasediments that were sheared. The discontinuities may correspond to decoupling levels/shear surfaces wrapping the low-strain area composed of metasediments with different competency and/or rheology contrast. Their formation was simultaneous with the shearing. The ductile deformed rocks recovered at Site U1504 were exhumed to the seafloor along a crustal-scale detachment fault (Figure 5c; Sun, Lin, et al., 2019). We therefore assume that the sheath folds forming at a similar midcrustal level were unroofed. Even though the presheath fold architecture is difficult to define, kinematics and style of sheath folds indicate that these structures formed in a pure-shear dominated regime, in which the material in the midcrust ductile field has the tendency to deform (distributed, flattening, and flow), however, confined at its top by a large, simple-shear fault during hyperextension (Figure 6c).

4.3. Rheology

The geometrical relationships between anastomosing decoupling levels, the mega-sheath folds and the extensional detachment fault on one hand and faults in the syn-rift sediments soling out in the detachment surface on the other hand suggest that these structures formed in the same overall phase of deformation. The lack of crustal-scale normal faults offsetting the top basement and the observation that the basement-sediment contact are sealed by early syn-rift sediments (Zhang et al., 2019; Figures 2, 3, and 4) show that these structures had to form during thinning and kept ongoing during hyperextension. In detail, the strain distribution was complex. While weak and prestructured metasedimentary layers were inherited in a forearc setting (Figure 6a), they are deformed predominantly by constriction/flattening as the material flow occurred during the early rifting stage (Figure 6b), the stronger and more brittle layers may have been offset during hyperextension along top-basement simple shear detachment faults (Figure 6c). As a consequence, the ductile midcrust was exhumed to this shallow level. These conditions can not only account for the formation of mega-sheath folds but also enable to make assumptions about the bulk rheology of the extending crust during hyperextension, which can be best explained as semiductile.

The source of heat that made sheath fold formation and the mylonitization below the detachment remains unconstrained. If slab rollback is considered to represent the onset of extension, the rollback is expected to be accompanied by a heat pulse related to inflowing hot material. Maybe it could have provided a heat source since the onset of the extension to account for the ductility during D1, and that may have continued into the phase of hyperextension, that is, laccolith intrusion of D2 folds. Thus, we interpret the mega-sheath folds to represent highly strained, attenuated ductile metasediments that deformed in a semiductile regime during hyperextension. The model of ductile deformation of metasediments established from the seismic basement flooring the hyperextended Liwan subbasin can probably extend further outboard, in particular, at the drilling area of IODP Sites U1504. This is supported by the occurrence of well-layered reflectors in the seismic basement and the lack of crustal-scale normal faults affecting highly thinned crust outboard the Liwan subbasin (Figure 1b).

In contrast to most rifted margins, where the hyperextension involves faulted blocks and brittle detachment faults (e.g., Boillot et al., 1980; Froitzheim & Manatschal, 1996; Peron-Pinvidic et al., 2013), the Liwan subbasin in the northern SCS shows a ductile rather than a brittle rheology of the hyperextended crust. Examples related to the exhumation of the middle-lower continental crust have been documented by Vissers et al. (1997), Jammes et al. (2009), and Clerc and Lagabrielle (2014) from the hyperextended domain in the North Pyrenean Zone in SW France. Manatschal et al. (2014) discussed the importance of compositional inheritance for the rheology of the extending crust. Using the example of the Liwan subbasin, we show that the occurrence of metasediments within the seismic basement can form locally very weak areas that can control the extensional processes and local architecture of rifted margins.

5. Conclusions

Sheath folds have been reported mainly from the outcrop to suboutcrop scale, in few examples also from the kilometer-seismic scale and referred to noncoaxial shear systems forming in the ductile field. In this study, crustal scale mega-sheath folds were mapped on 3-D seismic lines in the hyperextended Liwan seismic basement. The observation of mega-sheath folds provides constraints for the bulk rheology of the extending crust and enables to propose new mechanisms for the formation of hyperextended crust in strongly inherited metasediment bearing forearc settings. The sheath folds may be caused by shearing and decoupling in

weak, anisotropic inherited and prestructured metasediments. In this study, we show that metasedimentary units deriving from midcrustal levels of a former forearc were exhumed at the footwall of an extensional detachment fault. Shearing of the deeper, ductile crust together with the remove of brittle upper portions in the crust may account for the majority of crustal-scale thinning simultaneous to sedimentation. The occurrence of extremely weak and resultant ductile metasediments in the crust may explain the absence of normal faults penetrating the crust during hyperextension and the absence of tilted blocks as observed in the hyperextended crust flooring the Liwan subbasin in the northern margin of the SCS.

Acknowledgments

Seismic lines used for this study have been provided by the Shenzhen Branch of China National Offshore Oil Corporation (CNOOC) after personal request and are published with the permission of CNOOC. We are grateful to Christopher K. Morley for his valuable comments. The authors would like to thank the editor Claudio Faccenna and the reviewers Per Terje Osmundsen and Alex Webb for their thoughtful and constructive suggestions in improving this paper. This study was financially supported by the key program of NSFC (41730532), K.C. Wong Education Foundation (GJTD-2018-13), Key Special Project for Introduced Talents Team of Southern Marine Science and Engineering Guangdong Laboratory (GML2019ZD0205), Science and Technology Program of Guangzhou (201804010371), NSFC Program (41576070, 41830537, and 41576041), and Guangdong NSF research team project (2017A030312002). Seismic data used in this work were provided in Figshare (<https://doi.org/10.6084/m9.figshare.12249794.v1>) for research purposes. The research used samples and data produced by the International Ocean Discovery Program (IODP).

References

- Alsop, G. I., & Holdsworth, R. E. (2006). Sheath folds as discriminators of bulk strain type. *Journal of Structural Geology*, *28*, 1588–1606. <https://doi.org/10.1016/j.jsg.2006.05.005>
- Alsop, G. I., Holdsworth, R. E., & McCaffrey, K. J. W. (2007). Scale invariant sheath folds in salt, sediments and shear zones. *Journal of Structural Geology*, *29*, 1585–1604. <https://doi.org/10.1016/j.jsg.2007.07.012>
- Boillot, G., Grimaud, S., Mauffret, A., Mougnot, D., Kornprobst, J., Mergoil-Daniel, J., & Torrent, G. (1980). Ocean-continent boundary off the Iberian margin: A serpentinite diapir west of the Galicia Bank. *Earth and Planetary Science Letters*, *48*(1), 23–34. [https://doi.org/10.1016/0012-821X\(80\)90166-1](https://doi.org/10.1016/0012-821X(80)90166-1)
- Carreras, J., Estrada, A., & White, S. (1977). The effects of folding on the C-axis fabrics of a quartz-mylonite. *Tectonophysics*, *39*, 3–24. [https://doi.org/10.1016/0040-1951\(77\)90085-3](https://doi.org/10.1016/0040-1951(77)90085-3)
- Clerc, C., & Lagabrielle, Y. (2014). Thermal control on the modes of crustal thinning leading to mantle exhumation. Insights from the Cretaceous Pyrenean hot paleomargins. *Tectonics*, *33*, 1340–1359. <https://doi.org/10.1002/2013TC003471>
- Clerc, C., Lahfid, A., Monié, P., Lagabrielle, Y., Chopin, C., Poujol, M., et al. (2015). High-temperature metamorphism during extreme thinning of the continental crust: A reappraisal of the north Pyrenean passive paleomargin. *Solid Earth, European Geosciences Union*, *6*, 643–668. <https://doi.org/10.5194/se-6-643-2015>
- Ez, V. (2000). When shearing is a cause of folding. *Earth-Science Reviews*, *51*, 155–172. [https://doi.org/10.1016/S0012-8252\(00\)00020-9](https://doi.org/10.1016/S0012-8252(00)00020-9)
- Fan, C., Xia, S., Cao, J., Zhao, F., Sun, J., Wan, K., & Xu, H. (2019). Lateral crustal variation and post-rift magmatism in the northeastern South China Sea determined by wide-angle seismic data. *Marine Geology*, *410*, 70–87. <https://doi.org/10.1016/j.margeo.2018.12.007>
- Fiduk, J. C., & Rowan, M. G. (2012). Analysis of folding and deformation within layered evaporites in Blocks BM-S-8 & -9, Santos Basin, Brazil. In G. I. Alsop, S. G. Archer, A. J. Hartley, N. T. Grant, & R. Hodgkinson (Eds.), *Salt Tectonics, Sediments and Prospectivity* (Vol. 363, pp. 471–487). London: Geological Society, London, Special Publications.
- Froitzheim, N., & Manatschal, G. (1996). Kinematics of Jurassic rifting, mantle exhumation, and passive-margin formation in the Austroalpine and Penninic nappes (eastern Switzerland). *Geological Society of America Bulletin*, *108*(9), 1120–1133. [https://doi.org/10.1130/0016-7606\(1996\)108<1120:KOJRM>2.3.CO;2](https://doi.org/10.1130/0016-7606(1996)108<1120:KOJRM>2.3.CO;2)
- Hall, R. (1996). Reconstructing Cenozoic SE Asia. In R. Hall, & D. J. Blundell (Eds.), *Tectonic evolution of Southeast Asia* (Vol. 106, pp. 203–224). London: Geological Society, London, Special Publications.
- Hart, N. R., Stockli, D. F., Lavie, L., & Hayman, N. W. (2017). Thermal evolution of a hyperextended rift basin, Mauléon Basin, western Pyrenees. *Tectonics*, *36*, 1103–1128. <https://doi.org/10.1002/2016TC004365>
- Holloway, N. H. (1982). North Palawan Block, Philippines: its relation to Asian Mainland and role in evolution of South China Sea. *American Association of Petroleum Geologists Bulletin*, *66*, 1355–1383. <https://doi.org/10.1306/03B5A7A5-16D1-11D7-8645000102C1865D>
- Hu, W., Hao, T., Jiang, W., Xu, Y., Zhao, B., & Jiang, D. (2015). An integrated geophysical study on the Mesozoic strata distribution and hydrocarbon potential in the South China Sea. *Journal of Asian Earth Sciences*, *111*, 31–43. <https://doi.org/10.1016/j.jseas.2015.05.015>
- Jammes, S., Manatschal, G., Lavie, L., & Masini, E. (2009). Tectonosedimentary evolution related to extreme crustal thinning ahead of a propagating ocean: Example of the western Pyrenees. *Tectonics*, *28*, TC4012. <https://doi.org/10.1029/2008TC002406>
- Lacassin, R., & Mattauer, M. (1985). Kilometre-scale sheath fold at Mattmark and implications for transport direction in the Alps. *Nature*, *316*, 739–742. <https://doi.org/10.1038/315739a0>
- Larsen, H. C., Jian, Z., Alvarez Zarikian, C. A., Sun, Z., Stock, J. M., Klaus, A., et al. (2018a). Site U1501. In Sun, Z., Jian, Z., Stock, J. M., Larsen, H. C., Klaus, A., Alvarez Zarikian, C. A., & the Expedition 367/368 Scientists, South China Sea Rifted Margin. In *Proceedings of the International Ocean Discovery Program*, 367/368. College Station, TX: International Ocean Discovery Program.
- Larsen, H. C., Jian, Z., Alvarez Zarikian, C. A., Sun, Z., Stock, J. M., Klaus, A., et al. (2018b). Site U1504. In Sun, Z., Jian, Z., Stock, J. M., Larsen, H. C., Klaus, A., Alvarez Zarikian, C. A., Expedition 367/368 methods, South China Sea rifted margin. In *Proceedings of the International Ocean Discovery Program*, 367/368. College Station, TX: International Ocean Discovery Program.
- Larsen, H. C., Mohn, G., Nirrengarten, M., Sun, Z., Stock, J., Jian, Z., et al. (2018c). Rapid transition from continental breakup to igneous oceanic crust in the South China Sea. *Nature Geoscience*, *11*, 782–789. <https://doi.org/10.1038/s41561-018-0198-1>
- Lei, C., Alves, T. M., Ren, J., Pang, X., Yang, L., & Liu, J. (2019). Depositional architecture and structural evolution of a region immediately inboard of the locus of continental breakup (Liwan subbasin, South China Sea). *Geological Society of America Bulletin*, *131*(7–8), 1059–1074. <https://doi.org/10.1130/B35001.1>
- Lescoutre, R., Tugend, J., Brune, S., Masini, E., & Manatschal, G. (2019). Thermal evolution of asymmetric hyperextended magma-poor rift systems: Results from numerical modeling and Pyrenean field observations. *Geochemistry, Geophysics, Geosystems*, *20*, 4567–4587. <https://doi.org/10.1029/2019GC008600>
- Li, C. F., Zhou, Z. Y., Hao, H. J., Chen, H. J., Wang, J. L., Chen, B., & Wu, J. S. (2008). Late Mesozoic tectonic structure and evolution along the present-day northeastern South China Sea continental margin. *Journal of Asian Earth Science*, *31*, 546–561. <https://doi.org/10.1016/j.jseas.2007.09.004>
- Li, F., Sun, Z., & Yang, H. (2018). Possible spatial distribution of the Mesozoic volcanic arc in the present-day South China Sea continental margin and its tectonic implications. *Journal of Geophysical Research: Solid Earth*, *123*, 6215–6235. <https://doi.org/10.1029/2017JB014861>
- Li, J., Zhang, Y., Dong, S., & Johnston, S. T. (2014). Cretaceous tectonic evolution of South China: A preliminary synthesis. *Earth-Science Reviews*, *134*, 98–136. <https://doi.org/10.1016/j.earscirev.2014.03.008>

- Manatschal, G., Lavier, L., & Chenin, P. (2014). The role of inheritance in structuring hyperextended rift systems: Some considerations based on observations and numerical modeling. *Gondwana Research*, 27, 140–164. <https://doi.org/10.1016/j.gr.2014.08.006>
- Nirrengarten, M., Manatschal, G., Yuan, X. P., Kusznir, N. J., & Maillot, B. (2016). Application of the critical coulomb wedge theory to hyper-extended, magma-poor rifted margins. *Earth and Planetary Science Letters*, 442, 121–132. <https://doi.org/10.1016/j.epsl.2016.03.004>
- Peron-Pinvidic, G., Manatschal, G., & Osmundsen, P. T. (2013). Structural comparison of archetypal Atlantic rifted margins: A review of observations and concepts. *Marine and Petroleum Geology*, 43, 21–47. <https://doi.org/10.1016/j.marpetgeo.2013.02.002>
- Prucha, J. J. (1992). Zone of weakness concept: A review and evaluation. In M. J. Bartholomew, D. W. Hyndman, D. W. Mogk, & R. Mason (Eds.), *Basement Tectonics 8: Proceedings of the International Conferences on Basement Tectonics* (Vol. 2, pp. 83–92). Dordrecht: Springer.
- Ramsay, J. G., & Huber, M. I. (1987). *The techniques of modern structural geology, Volume 2: Folds and fractures*. London, UK: Academic Press.
- Reber, J. E., Dabrowski, M., & Schmid, D. W. (2012). Sheath fold formation around slip surfaces. *Terra Nova*, 24, 417–421. <https://doi.org/10.1111/j.1365-3121.2012.01081.x>
- Rosas, F. M., Marques, F. O., Luz, A., & Coelho, S. (2002). Sheath folds formed by drag induced by rotation of rigid inclusions in viscous simple shear flow: Nature and experiment. *Journal of Structural Geology*, 24, 45–55. [https://doi.org/10.1016/S0191-8141\(01\)00046-3](https://doi.org/10.1016/S0191-8141(01)00046-3)
- Ru, K., & Pigott, J. D. (1986). Episodic rifting and subsidence in the South China Sea. *American Association of Petroleum Geologists Bulletin*, 70, 1136–1155. <https://doi.org/10.1306/94886A8D-1704-11D7-8645000102C1865D>
- Ruan, A., Niu, X., Wu, Z., Wu, Z., & Xue, B. (2009). The 2D velocity and density structure of the Mesozoic sediments in the Chaoshan depression. *Geological Journal of China Universities*, 15, 522–528. <https://doi.org/10.1002/gj.2778>
- Schlüter, H. U., Hinz, K., & Block, M. (1996). Tectono-stratigraphic terranes and detachment faulting of the South China Sea and Sulu Sea. *Marine Geology*, 130, 39–78. [https://doi.org/10.1016/0025-3227\(95\)00137-9](https://doi.org/10.1016/0025-3227(95)00137-9)
- Searle, M. P., & Alsop, G. I. (2007). Eye to eye with a mega-sheath fold: a case study from Wadi Mayh, northern Oman Mountains. *Geology*, 35, 1043–1046. <https://doi.org/10.1130/G23884A.1>
- Shao, L., Cao, L., Qiao, P., Zhang, X., Li, Q., & van Hinsbergen, D. J. (2017). Cretaceous-Eocene provenance connections between the Palawan continental Terrane and the northern South China Sea margin. *Earth and Planetary Science Letters*, 477, 97–107. <https://doi.org/10.1016/j.epsl.2017.08.019>
- Shao, L., You, H., Hao, H., Wu, G., Qian, P., & Lei, Y. (2007). Petrology and depositional environments of Mesozoic strata in the northeastern South China Sea (in Chinese with English Abstract). *Geological Review*, 53, 1–6.
- Shi, H., & Li, C. F. (2012). Mesozoic and early Cenozoic tectonic convergence-to-rifting transition prior to opening of the South China Sea. *International Geology Review*, 54(15), 1801–1828. <https://doi.org/10.1080/00206814.2012.677136>
- Sun, L., Sun, Z., Huang, X., Jiang, Y., & Stock, J. M. (2019). Microstructures documenting Cenozoic extension processes in the northern continental margin of the South China Sea. *International Geology Review*. <https://doi.org/10.1080/00206814.2019.1669079>
- Sun, X., Zhang, X., Zhang, G., Lu, B., Yue, J., & Zhang, B. (2014). Texture and tectonic attribute of Cenozoic basin basement in the northern South China Sea. *Science in China Series D-Earth Sciences*, 57, 1199–1211. <https://doi.org/10.1007/s11430-014-4835-2>
- Sun, Z., Lin, J., Qiu, N., Jian, Z. M., Wang, P. X., Pang, X., et al. (2019). The magmatism in the thinning and breakup process of the South China Sea continental margin. *National Science Review*, mwz116. <https://doi.org/10.1093/nsr/nwz116>
- Sun, Z., Zhou, D., Zhong, Z., Xia, B., Qiu, X., Zeng, Z., & Jiang, J. (2006). Research on the dynamics of the South China Sea opening: Evidence from analogue modeling. *Science in China Series D: Earth Sciences*, 49, 1053–1069. <https://doi.org/10.1007/s11430-006-1053-6>
- Vacherat, A., Mouthereau, F., Pik, R., Bernet, M., Gautheron, C., Masini, E., et al. (2014). Thermal imprint of rift-related processes in orogens as recorded in the Pyrenees. *Earth and Planetary Science Letters*, 408, 296–306. <https://doi.org/10.1016/j.epsl.2014.10.014>
- Vissers, R. L. M., Drury, M. R., Newman, J., & Fliervoet, T. F. (1997). Mylonitic deformation in upper mantle peridotites of the north Pyrenean zone (France): Implications for strength and strain localization in the lithosphere. *Tectonophysics*, 279(1–4), 303–325. [https://doi.org/10.1016/S0040-1951\(97\)00128-5](https://doi.org/10.1016/S0040-1951(97)00128-5)
- Wu, G. X., Wang, R. J., Hao, H. J., & Shao, L. (2007). Microfossil evidence for development of marine Mesozoic in the north of South China Sea (in Chinese with English abstract). *Marine Geology and Quaternary Geology*, 27, 79–85.
- Yan, P., Wang, L., & Wang, Y. (2014). Late Mesozoic compressional folds in Dongsha Waters, the northern margin of the South China Sea. *Tectonophysics*, 615, 213–223. <https://doi.org/10.1016/j.tecto.2014.01.009>
- Yan, P., Zhou, D., & Liu, Z. (2001). A crustal structure profile across the northern continental margin of the South China Sea. *Tectonophysics*, 338, 1–21. [https://doi.org/10.1016/S0040-1951\(01\)00062-2](https://doi.org/10.1016/S0040-1951(01)00062-2)
- Yang, L., Ren, J., McIntosh, K., Pang, X., Lei, C., & Zhao, Y. (2018). The structure and evolution of deepwater basins in the distal margin of the northern South China Sea and their implications for the formation of the continental margin. *Marine and Petroleum Geology*, 92, 234–254. <https://doi.org/10.1016/j.marpetgeo.2018.02.032>
- Yao, B., Zeng, W., Hayes, D. E., & Spangler, S. (1994). *The geological memoir of South China Sea surveyed jointly by China and USA* (p. 204). Wuhan: China University of Geosciences Press. (in Chinese)
- Ye, Q., Mei, L., Shi, H., Camanni, G., Shu, Y., Wu, J., et al. (2018). The late cretaceous tectonic evolution of the South China Sea area: An overview, and new perspectives from 3D seismic reflection data. *Earth-Science Reviews*, 187, 186–204. <https://doi.org/10.1016/j.earscirev.2018.09.013>
- Zahirovic, S., Seton, M., & Müller, R. D. (2014). The Cretaceous and Cenozoic tectonic evolution of Southeast Asia. *Solid Earth Discussions*, 5, 1335–1422. <https://doi.org/10.5194/se-5-227-2014>
- Zhang, C., Su, M., Pang, X., Zheng, J., Liu, B., Sun, Z., & Manatschal, G. (2019). Tectono-sedimentary analysis of the hyperextended Liwan Sag Basin (Midnorthern margin of the South China Sea). *Tectonics*, 38, 470–491. <https://doi.org/10.1029/2018TC005063>
- Zhou, D., Ru, K., & Chen, H. Z. (1995). Kinematics of Cenozoic extension on the South China Sea continental margin and its implications for the tectonic evolution of the region. *Tectonophysics*, 251, 161–177. [https://doi.org/10.1016/0040-1951\(95\)00018-6](https://doi.org/10.1016/0040-1951(95)00018-6)
- Zhou, D., Wang, W., Wang, J., Pang, X., Cai, D., & Sun, Z. (2006). Mesozoic subduction accretion zone in northeastern South China Sea inferred from geophysical interpretations. *Science in China Series D-Earth Sciences*, 49, 471–482. <https://doi.org/10.1007/s11430-006-0471-9>
- Zuber, M. T., Parmentier, E. M., & Fletcher, R. C. (1986). Extension of continental lithosphere—A model for two scales of basin and range deformation. *Journal of Geophysical Research*, 91, 4826–4838. <https://doi.org/10.1029/JB091iB05p04826>